13th Australasian Fluid Mechanics Conference
Monash University, Melbourne, Australia
13-18 December 1998

AN EXPERIMENTAL INVESTIGATION OF THE FLUID FLOW CLOSE TO A MOVING SOLID BOUNDARY

G.D. RIGBY[1], C.D. RIELLY[2], J.A. LUCAS[1], G.M. EVANS[1] and L. STREZOV[3]

[1]Department of Chemical Engineering
University of Newcastle, Callaghan, NSW, 2308, AUSTRALIA

[3] BHP Research Newcastle Laboratories
P.O. Box 188, Wallsend, NSW, 2287, AUSTRALIA

ABSTRACT

An experimental study has been conducted to measure the flow field in the vicinity of a moving solid boundary which passes through a free surface into a liquid phase. Through the use of PIV and pulsed hydrogen bubble generation techniques, the bulk bath recirculation velocity and the variation in the liquid velocity field in the vicinity of the three-phase contact line have been quantified for solid boundary velocities ranging between 0.04 and 0.16 m s^{-1}.

INTRODUCTION

Many industrial processes involve passing a wire, strip or roller through the free surface of a liquid. One such example is the coating of steel plate with zincalume in a continuous strip coating bath. The nature of the chemical bonding of the plate to the overlay ultimately determines the quality of the product and therefore it is essential to understand all the factors influencing its formation. These include mass transfer, heat transfer, and wettability.

Previous studies have shown that the thickness, nature and uniformity of the inter-metallic alloy layer is dependent on the process conditions present when the initial contact between the steel strip and the molten coating occurs (Guttmann, 1994; Richards *et al.*, 1994). A large body of work has been conducted for long contact times (*i.e.* 5 seconds); however, recent high speed dip coating experiments (Zhou *et al.*, 1995) have suggested that the wetting of the strip by the molten metal and the subsequent growth of the intermetallic layer is determined prior to the first 20 ms of contact. Therefore, an understanding of the flow in the immediate vicinity of the entry of the plate into the bath is important.

There have been many attempts at modelling the flow near a moving contact line under conditions of creeping flow. The original solution of Moffat (1964) demonstrates the difficulties, with classical assumptions resulting in unbounded stresses near the contact line. Various assumptions, including slip against the solid surface on a microscopic scale (Dussan, 1976; Hocking, 1977) have been introduced to relieve this anomaly.

[2] On leave from Department of Chemical Engineering, Cambridge University, Pembroke Street, Cambridge, CB2 3RA, U.K..

A recent experimental study (Chen *et al.*, 1997) has investigated the flow field under creeping flow conditions, finding good agreement with the modulated wedge solution of Cox (1986). To date however, there is little data concerning conditions which are similar to those found in an industrial coating bath. In these devices, there is a significantly higher Reynolds number for the flow in the vicinity of the roller, based on the meniscus length scale, than that of Chen *et al.* (1997).

In this study, pulsed hydrogen bubble generation and particle image velocimetry (PIV) techniques are used to interrogate the flow generated in a water bath by a rotating, partially submerged, dried roller. The experimental conditions approximate those found in an industrial coating bath, due to the dynamic similarity which results from similar viscosities for water and the molten zincalume. The investigation focuses attention on the region close to the three-phase contact line between the plunging roller surface, the gas above the free surface, and the liquid within the bath.

EXPERIMENTAL METHOD

Apparatus

The experimental investigation was conducted within a stainless steel framed tank of rectangular cross-section, with sides constructed from either transparent polycarbonate or glass (see Fig. 1).

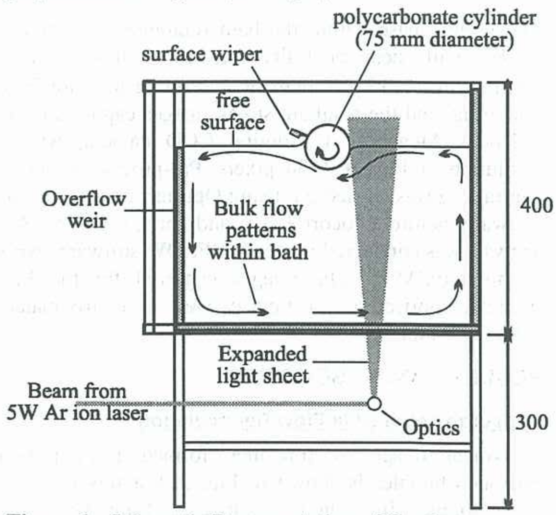

Figure 1 : Schematic Representation of Coating Apparatus

From Fig. 1 it can be seen that the maximum liquid level within the tank is set by an overflow weir, which is level with the horizontal axis of the roller. To minimise free surface vibration when operating at lower surface velocities, the roller is driven by a 0.5 kW dc variable speed motor, which is connected through a 6:1 stepped pulley arrangement. The surface of the roller is wiped during rotation to remove any surface liquid and prevent carry-over. A representation of the general expected flow patterns within the bath and free surface profile during operation, is also shown in the figure.

Measurement Techniques

Hydrogen Bubble Visualisation

During operation of the roller apparatus there is a bulk recirculating fluid motion around the confining walls of the bath. To quantify the effect of roller speed on this recirculation, hydrogen bubble visualisation experiments were carried out to determine average fluid velocities close to the free surface. For these experiments, the hydrogen-generating cathode probe was placed in the horizontal plane, at distances ranging from 10 to 100 mm from the leading edge of the roller, and at submersion depths of 1, 5, and 10mm below the free surface. The pulsed lines of hydrogen bubbles were observed using the CCD camera, positioned above the free surface. Subsequent analysis of the captured digital images was carried out using Optimas V 6.0 image analysis software (Optimas Corp. Bothell, WA, USA). From these experiments a background measure was obtained of fluid movement within the bath.

Particle Image Velocimetry

To measure the velocity field in the vicinity of the contact point between the roller and the fluid bath, PIV analysis was used to provide instantaneous velocity data over a two-dimensional plane, perpendicular to the roller surface. Laser illumination, provided by a Spectra Physics 5 W continuous-wave argon-ion laser, was passed through an acousto-optic modulator and pin hole arrangement to produce a pulsed light source. Following this, the beam was redirectred with a beam-steering mirror and expanded using cylindrical lens optics to produce a final laser sheet with a thickness of approximately 3 mm.

The liquid phase within the bath (deionised water) was seeded with near neutrally buoyant hollow ceramic spheres (dia. = 12 μm; density = 1100 kg m^{-3}) for light scattering, and the resultant streak images captured using a Kodak Megaplus 1.4 digital CCD camera, with a resolution of 1316 x 1034 pixels. Pre-processing image contrasting was carried out using Optimas image analysis software, before autocorrelation and particle pairing PIV analysis was conducted using VISIFLOW software (AEA Technology,1997). The images captured for the PIV studies comprised a total field of view of approximately 8 mm by 9 mm.

RESULTS AND DISCUSSION

Measurement of Bulk Flow Recirculation

A typical image of timelines formed from pulsed hydrogen bubbles is shown in Fig. 2. For this figure, a fine platinum wire cathode was located 10 mm below the free surface and centrally between the bath side walls.

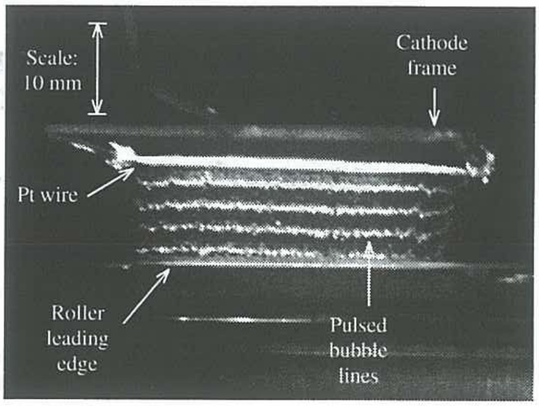

Figure 2 : Typical H_2 Pulsed Bubble Visualisation Image ($U_T = 0.26$ ms^{-1}, $\Delta t = 500$ ms).

Similar images were also obtained for distances up to 100 mm from the roller surface.

Figure 3 shows a comparison of the horizontal fluid velocity as a function of the distance from leading edge of the roller and at various depths, *h*, below the free surface.

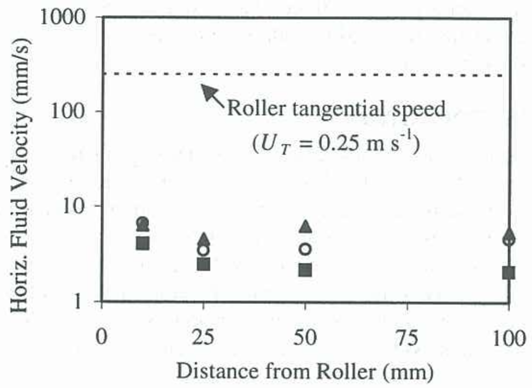

Figure 3 : Bulk Recirculation Velocity in Bath
Legend: (■, *h* = 1 mm; O, 5 mm; ▲, 10 mm).

From Fig. 3, two points can be made: firstly there is generally little variation in the fluid velocity with distance from the roller for the submersion depths of (*h* = 5, 10 mm). Secondly, for the fluid layers closer to the gas/liquid interface (represented by the data for *h* = 1 mm), the fluid is travelling toward the roller at a velocity which is generally only half of that found in the deeper layers (*i.e.* $5 < h < 10$ mm), indicating that there is a velocity gradient projecting from just below the free surface down into the liquid. This result can be contrasted with the results from the creeping flow model (Moffat, 1964) which predicts a constant free surface velocity which is approximately $0.6U_T$.

Similar observations have also been made for all roller speeds increasing to $U_T = 1.0$ m s^{-1}.

Measurement of Flow Approaching Roller

The observations from pulsed hydrogen bubble experiments have shown that despite the confining walls of the visualisation model bath, significant acceleration of liquid by the roller occurs only within a small region in close proximity to the surface of the roller. In order to gain some understanding of the size of this region of influence, experiments were conducted using PIV techniques to visualise the flow within a vertical plane normal to the rotational axis of the roller. To maximise the contrast from the light scattered by seeding particles within the laser sheet, the plane of illumination was located at a distance equal to one quarter of the width from the front face of the bath.

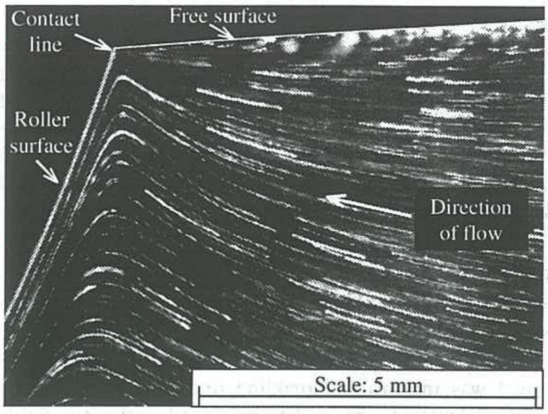

Figure 4 : Visualisation of Flow Adjacent to Roller ($U_T = 0.12$ m s^{-1})

The image shown in Fig. 4 was obtained by providing a continuous sheet of laser illumination, allowing the visualisation of streaklines within the liquid. As shown in the figure, there is a small depression of the free surface as the liquid approaches the contact line with the roller.

Perhaps the most striking feature of this flow is the way in which the liquid is drawn upward toward the contact line before experiencing rapid downward acceleration during entrainment into the fluid boundary layer associated with the moving roller.

The consequence of the upward fluid flow towards the initial solid/liquid contact line is the formation of a distinct region of relatively stagnant liquid in the fluid layers immediately below the free surface. This region appears to begin at the contact line and increase in depth with increasing distance along the free surface away from the roller. Similar flow patterns to that shown in Fig. 4 have been seen for all experimental roller velocities rising to $U_T = 1.0$ m s^{-1}.

Figure 5 shows a PIV streak image obtained using a three pulse laser illumination and following pre-processing with local smoothing routines. The image is typical of all roller speeds considered in this study. For the particular image shown, the laser exposure time was set to produce a correct three-pulse streak length to allow the measurement of fluid velocities in the bulk of the liquid.

It can also be seen from Fig. 5 that the selected laser pulse duration was unsuitable for the capture of streak patterns in the separate fluid regions adjacent to the roller and close to the free surface. In the fast-moving boundary layer region next to the roller, the captured streaks were too long to be contained within the auto-correlation windows, whilst the fluid in the free surface region was travelling too slowly to allow adequate pixel separation between the individual pulses.

As a result, for each roller speed, it was necessary to perform a series of image capture routines at significantly different exposure times to ensure that the fluid velocity in each region of the flow was sufficiently resolved after ensemble (post processing) averaging of the separate files.

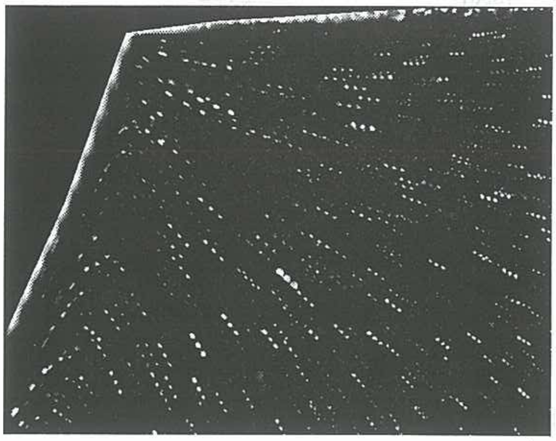

Figure 5 : Typical PIV Input Data File, $U_T = 0.04$ m s^{-1}. (Laser pulse separation = 33 ms)

The resultant velocity vector plots obtained from the PIV analysis are shown in Figs. 6 to 9. Calculated streamlines for the flow field are also shown and for comparison purposes, a constant length for the reference vector has been maintained throughout the figures.

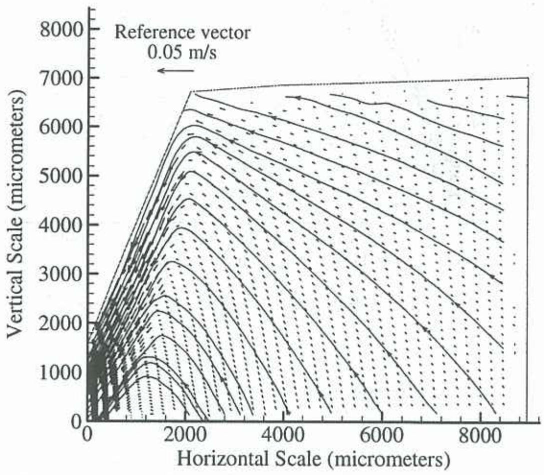

Figure 6 : Velocity Field in Flow for $U_T = 0.04$ m s^{-1}

From Figs. 6 to 9, it can firstly be noticed that the velocity at all regions within the liquid is increased as the roller speed increases. The indicated streamline pattern for the flows matches that shown by the streaklines of the continuous visualisation image in Fig. 4.

For all roller velocities, the flow is drawn upwards towards the free surface and the three-phase contact line before entering the rapidly downflowing boundary layer. At higher roller speeds, the streamlines show that a larger horizontal velocity is present in the bulk liquid region approaching the roller, than that of the lower roller speeds where the approaching flow has a larger vertical velocity component.

It can also be seen from Figs. 6 to 9 that at higher roller speeds the thickness of the liquid boundary layer on the rotating roller becomes thinner as the roller speed is increased.

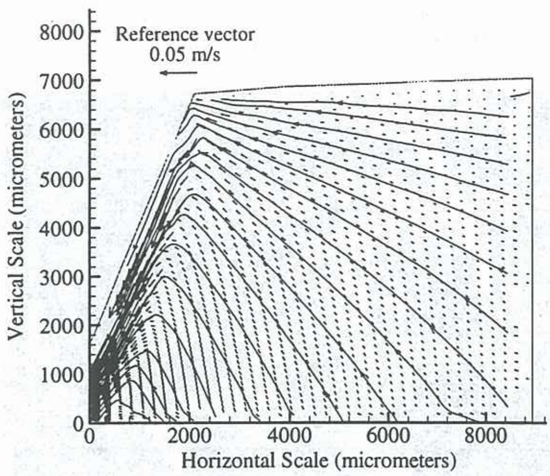

Figure 7 : Velocity Field in Flow for $U_T = 0.08$ m s^{-1}

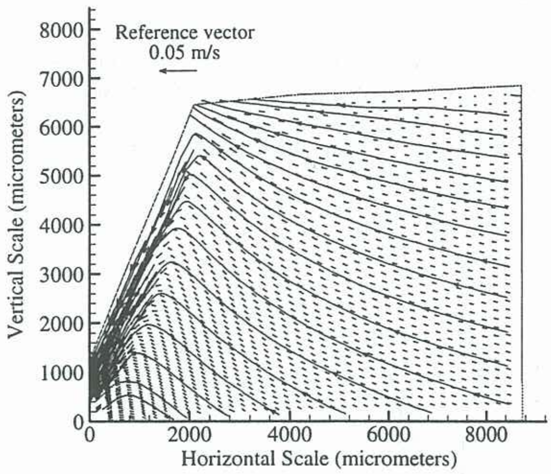

Figure 8 : Velocity Field in Flow for $U_T = 0.12$ m s^{-1}

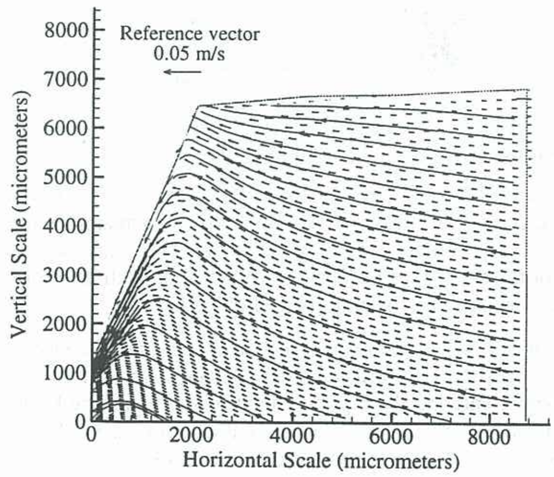

Figure 9 : Velocity Field in Flow for $U_T = 0.16$ m s^{-1}

Future work is continuing to attempt to resolve the structure of the flow within the liquid boundary layer adjacent to the roller in greater detail. These results are expected to also assist in the validation of theoretical model currently under development (Sciffer *et al.*, 1998).

CONCLUSIONS

Experiments are described for the measurement of the liquid flow patterns generated by a rotating, dried roller, which is partially submerged within a water bath.

For a range of roller velocities up to 1 m s^{-1}, hydrogen bubble visualisation studies showed that the bulk recirculation velocity within the bath was seen to be moving continuously towards the roller at less than 3% of the tangential roller speed. This progress continued until a region adjacent to the roller was reached where rapid acceleration of liquid occurred and depression of the liquid meniscus could be observed. These experimental also showed that just below the free surface, the liquid velocity was travelling at a significantly slower rate than the fluid layers several millimetres below.

Particle image velocimetry measurements of the flow region in the vicinity of the three-phase contact line revealed the presence of a fast, downward-moving boundary layer, which decreased in thickness as the roller speed was increased. Streakline images and streamline plots calculated from the measured velocity fields showed that the boundary layer was fed by a upward flow towards the contact line.

The results obtained are expected to be of use in the validation of theoretical models for the prediction of liquid flow close to moving solid boundaries, and may also assist in the understanding of the operating behaviour of industrial systems, such as coating systems where a three-phase contact line is present.

NOMENCLATURE

h	Liquid depth below free surface	m
U_T	Roller tangential velocity	m s^{-1}
Δt	H_2 bubble space time	ms

REFERENCES

AEA Technology, "VISIFLOW system user manual", AEA Technology plc, Harwell, Didcot, U.K., 1997.

CHEN, Q., RAMÉ, E. and GAROFF, S., "The velocity field near moving contact lines", *J. Fluid Mech.*, **337**, 49–66, 1997.

COX, R.G., "The dynamics of the spreading of liquids on a solid surface. Part 1. Viscous flow", *J. Fluid Mech.*, **168**, 169–194, 1986.

DUSSAN, E.B., "The moving contact line: the slip boundary condition", *J. Fluid Mech.*, **77**, 665-689, 1976.

GUTTMANN, M., "Diffusive phase transformations in hot dip galvanising", *Materials Sci. Forum*, **155/156**, 527–548, 1994.

HOCKING, L.M., "A moving fluid interface. Part 2. The removal of the force singularity by a slip flow", *J. Fluid Mech.*, **79**, 209, 1977.

MOFFAT, H.K., "Viscous and resistive eddies near a sharp corner", *J. Fluid Mech*, **18**, 1–18, 1964.

RICHARDS, R.W., JONES, R.D., CLEMENTS, P.D. and CLARKE, H., "Metallurgy of continuous hot dip aluminising", *Int. Materials Rev.*, **39**, 5, 191–212, 1994.

SCIFFER, S.D., STREZOV, L., EVANS, G.M. and LUCAS, J.A., "Hydrodynamic meniscus profiles in creeping flow", *Chem. Eng. Sci.*, 1998, in press.

ZHOU, Z.F, TIDEN, G.M., LIU, Q.Y., MERCER, P.D. and WILLIS, D.J., "The formation and growth of the interfacial alloy layer in Zn-55% Al-1.5% Si hot-dipped coatings", *Galvatech 95 Conf. Proc.*, Chicago, 289–293, 1995.